# Highly Efficient Destruction of Perchlorate to Nontoxic Chloride Ion ($Cl^-$) from Aqueous Solutions by Bimetallic Fe/Ni Nanoparticles

***Zarei, Ali Reza****[+]***; Moloudi, Ali***

*Faculty of Chemistry and Chemical Engineering, Malek Ashtar University of Technology, P.O. Box 15875-1774 Tehran, I.R. IRAN*

**ABSTRACT:** *In this work, stabilized Ni/Fe bimetallic nanoparticles (S-Ni/Fe NPs) were synthesized in the presence of starch as the stabilizing agent and characterized by FE-SEM, EDS, and XRD. The results showed that the S-Ni/Fe NPs were spherical in the shape and have a nearly uniform distribution with a particle size of 20-50 nm. Then, perchlorate as a persistent inorganic pollutant was destructed to chloride ion by the S-Ni/Fe NPs. The main factors controlling the removal of perchlorates, such as the initial pH of the solution, the dosage of the S–Fe/Ni NPs, initial perchlorate concentration, temperature, and reaction time were optimized by using an experimental design based on response surface methodology. Under the optimal conditions, perchlorate was destructed with an efficiency of nearly 100%. The kinetics for the destruction of perchlorate by the S-Ni/Fe NPs complied with pseudo-first-order characteristics. The rate constant ($K_{obs}$) and activation energy ($E_a$) for the destruction were obtained 0.0471 1/min at 343 K and 13.07 kJ/mol, respectively. Therefore, the present study offers a powerful bimetallic nanoparticle for the destruction of the environmental oxidant pollutants such as perchlorate from aqueous media.*

**KEYWORDS:** *Perchlorate; Destruction; Persistent inorganic pollutants; Bimetallic nanoparticles.*

## INTRODUCTION

The persistent inorganic pollutants (PIPs) are inorganic compounds that are resistant to destruction through chemical, biological, and photolytic processes, and are stable in the environment [1]. These pollutants including oxyanions, mineral acids, sulfates, some of organometallic complexes, and cyanides that are non-biodegradable and persist in the environment [2]. Perchlorate ($ClO_4^-$) as an oxyanion has recently received a great deal of attention due to high concentrations found in ground waters and surface waters. Perchlorate primarily has been released to the environment via use of Ammonium Perchlorate (AP) as a propellant in missiles, rockets, and explosives, as a pyrotechnic in fireworks, in magnesium batteries, paint, and as an automobile air bag inflator [3, 4]. The important source of AP is the demulsion and recovery of the propellant from solid rocket motors, which can result in contamination of AP in the soil, the surface water, and the groundwater. Perchlorate is a harmful matter to health because it reduces the absorption of iodine by thyroid hormone production decreases [5]. A perchlorate reference

* *To whom correspondence should be addressed.*
*+ E-mail: zarei1349@gmail.com*
*1021-9986/2021/1/57-68 12/$/6.02*

dose to 0.0007 mg/kg/day in the drinking water is the no-observed-effect level (NOEL) that proposed by the National Academy of Science, USA. This is equivalent to 24.5 µg/L in the drinking water (drinking water equivalent level, DWEL) [6].

As a strong oxidant with a higher oxidation state of the chlorine, +7, the perchlorate reduction is a thermodynamically desirable process under environment conditions [3].

$$ClO_4^- + 8H^+ + 8e^- \rightarrow Cl^- + 4H_2O \qquad E° = +1.29\ V \qquad (1)$$

Because of the high reduction potential of perchlorate, it is an electron acceptor in the presence metal nanoparticles, which often highly depend on the structure of the NPs (e.g., shape, size, composition, and surface chemistry) [7]. The nanometals used for these purpose include iron and zinc nanoparticles ($Fe^0$ or $Zn^0$), however nanoscale zero valent iron (nZVI) is most commonly used [8-12].

Besides, other metals such as nickel and palladium have been added to improve the reductive destruction rate. The combination of nZVI with a noble metal is referred to bimetallic nanoparticles. The iron-noble metal couple essentially creates numerous galvanic cells where iron serves as the anode and becomes preferably oxidized. Meanwhile, the noble metal (cathode) is protected and remains unchanged. Bimetallic NPs, also called nanoalloys, are a class of important materials receiving considerable attention because of their unique properties. Bimetallic NPs typically consist of a metal such as iron as electron donors and second metal (such as nickel, palladium, etc.) as an activator [13]. In many cases, the specific properties of bimetallic NPs are enhanced because of the synergistic effects of the two distinct metals. Moreover, the diversity in structures, compositions, and properties of bimetallic NPs enable their widespread application in various fields such as catalyst [14], electrochemistry [15, 16], magnetism [17, 18], optics, and biomedicine [12].

Because zero-valent metals-based reactions are surface mediated processes, increasing the surface area of nano zero-valent metals (nZVM) was found to increase the reaction rate. It has been shown that decreasing the size of zero-valent metallic particles to the nanoscale can greatly enhance the reaction rates [19]. However, because nanoscale zero-valent metals tend to agglomerate rapidly. Therefore, the nZVM without a stabilizer is agglomerated to large particles. To prevent agglomeration and also to stabilize metal nanoparticles, various stabilizers have been reported [20-24]. Compared with conventional non-stabilized nZVM, the stabilized nanoparticles displayed much greater surface area, superior physical stability, and faster reaction rates. The water-soluble starch, sodium carboxyl methylcellulose (CMC), and chitosan are widely used as a stabilizer [25-27].

So far, In recent years, the various treatment technologies have been applied for removal of perchlorate from water including biological removal [28, 29], Ion Exchange (IX) [30], tailored activated carbon adsorption [31], filtration [32], and chemical reduction [33-35]. All of these methods, only transferred perchlorate from aqueous phase to solid phase, but do not degradation. In the reduction methods by metal nanoparticles, the complete degradation occurs. The studies have also been conducted to investigate the reduction of perchlorate by iron metal. Thermodynamics predicts that perchlorate should be readily transformed to chloride ion in the presence of metals such as ZVI; however, recent researches demonstrated that perchlorate reduction by $Fe^0$ is a very slow process under ambient conditions [36]. The purpose of this study is to propose a fast method and high efficiency for the removal of perchlorate via reductive destruction by metal nanoparticles. In this study, we evaluated the feasibility of the S-Ni/Fe NPs for the destruction of perchlorate and investigated the reaction kinetics and the factors affecting the destruction rates during treatment.

## EXPERIMENTAL SECTION

### *Reagents and instruments*

All the chemicals and reagents, which are used in this work, were in analytical grade. Sodium borohydride ($NaBH_4$, 98%) was purchased from Fluka. Starch ($(C_{12}H_{22}O_{11})_n$, >99%), ferrous chloride ($FeCl_2.4H_2O$, >99%), Nickel (II) acetate hexahydrate (Ni $(acetate)_2 \cdot 6H_2O$, >99%), ammonium perchlorate ($NH_4ClO_4$, >99%), hydrochloric acid (HCl), sodium hydroxide (NaOH), methylene blue, sulfuric acid ($H_2SO_4$) and chloroform ($CHCl_3$) purchased from Merck (Merck, Darmstadt, Germany). In all of the experiments, deionized water was used to prepare solutions.

A Hitachi model 3310 UV-Vis spectrophotometer with 1 cm quartz cells was used for recording absorbance spectra.

A pH meter (PH.Z.S. PTR79) was used to measure pH. FE-SEM images were acquired using an electron microscopy Sigma model (Zeiss Ltd. Co., Germany). The XRD analysis was carried out using a Model STOE STADI Diffractometer. (STOE Ltd. Co., Germany). Samples were analyzed by ion chromatography using Professional IC 850 fitted with a conductivity detector (METROHM AG, Swiss).

***Preparation of the S-Ni/Fe NPs***

The S–Fe/Ni NPs were synthesized using the liquid-phase reduction method with starch as a stabilizer material, which has been previously reported [13]. The co-precipitation method was performed by dissolving a mixture of starch (0.5 g), $Ni(acetate)_2 .4H_2O$ (0.224 g), and $FeCl_2.4H_2O$ (5.964 g) in 50 mL deionized water into a three-necked flask of 200 mL volume and stirring well with mechanic stirrer (Ni:Fe with 1:33 molar ratio). Separately, 50 mL of 3 mol/L $NaBH_4$ solution was added into a 100 mL dropper. The reaction was initiated by dropwise excess $NaBH_4$ solution into metals ions solution (within 2 hours). Nitrogen gas was continuously flowed to prevent the oxidation of freshly the prepared NPs. The proposed chemical reactions for the preparation of S-Ni/Fe NPs are as follows:

$$2Fe^{2+}_{(aq)} + BH^{-}_{4(aq)} + 3H_2O_{(l)} \rightarrow \quad (2)$$

$$2Fe^{\circ}_{(s)} + H_2BO^{-}_{3(aq)} + 4H^{+}_{(aq)} + 2H_{2(g)}$$

$$2Fe^{\circ}_{(s)} + Ni^{2+}_{3(aq)} + Fe^{2+}_{(aq)} + Ni^{\circ}_{(s)} \downarrow \quad (3)$$

A magnet was employed to collect the S–Ni/Fe particles and these were quickly rinsed three times with distilled water, and then dried at 70 °C under vacuum overnight, and kept in a nitrogen atmosphere before use. The theoretical mass fraction of starch in synthesized S–Fe/Ni was 1 (%wt), and the Ni:Fe molar ratio was 0.03. Based on experiments conducted in different periods, nanoparticles are usable in the presence of starch, up to a maximum of 30 days. Also, by increasing the percentage of nickel in comparison to iron in nanoparticles, the rate of corrosion of iron increases, and the nanoparticles are not usable for more than a few hours.

***Perchlorate destruction procedure***

A batch procedure was carried out for the destruction process. Under optimal conditions, first, in a three-necked flask, 50 mL solution of 10 µg/mL of perchlorate ($C_0$) purged under $N_2$ gas for 10 min, and the pH of the solution was adjusted at 5.6 using 0.1 mol/L $H_2SO_4$ and/or 0.1 mol/L NaOH. Following it, 63 mg of the S-Ni/Fe NPs was transferred to a flask and was washed three times with pure alcohol for removing starch coated on the Ni/Fe NPs. Then, the washed Ni/Fe NPs were added to the perchlorate solution and was stirred for 90 min at 70 $^0$C. Finally, the nanoparticles were separated using a strong magnet (1.2 Tesla). The concentration of perchlorate ($C_t$) in the stripped solution was determined spectrophotometrically according to the procedure described below. The entire scheme of preparation of S-Ni/Fe NPs and its application in reductive destruction of perchlorate was shown in Scheme 1.

***Spectrophotometric determination of perchlorate***

For the monitoring of the perchlorate, it was used from a simple spectrophotometric method based on the ion pairing of the perchlorate with the methylene blue in the acidic media and its extraction into chloroform [37]. Briefly, an aliquot of the perchlorate solution so that its final concentration would be in the range of 1.0-10 µg/mL, 1 mL of methylene blue (1.5 mmol/L), and 1 mL of sulfuric acid (2 mol/L) were transferred into a 10-mL centrifuge tube. Then, 3 mL of chloroform was added and was shaken for 5 min. The test tube was set aside for a 2 min to separate the organic phase from the aqueous phase, and the absorbance organic phase was measured at 676 nm. The linear calibration curve was obtained in the concentration range of 0.5 to 20 µg/mL and detection limit was 80 ng/mL. Destruction efficiency for perchlorate was calculated as follow:

$$\%DE = \frac{A_o - A_C}{A_o} \times 100\% \quad (4)$$

Where *DE* is the destruction efficiency (%) of perchlorate, $A_o$ and $A_c$ absorbance at the initial and appropriate times of the process, respectively.

***Design of the experiments***

The Response Surface Methodology (RSM) is a collection of the statistical and mathematical techniques useful for developing, improving, and optimizing processes. RSM defines the effect of the independent variables, alone or in combination, on the process.

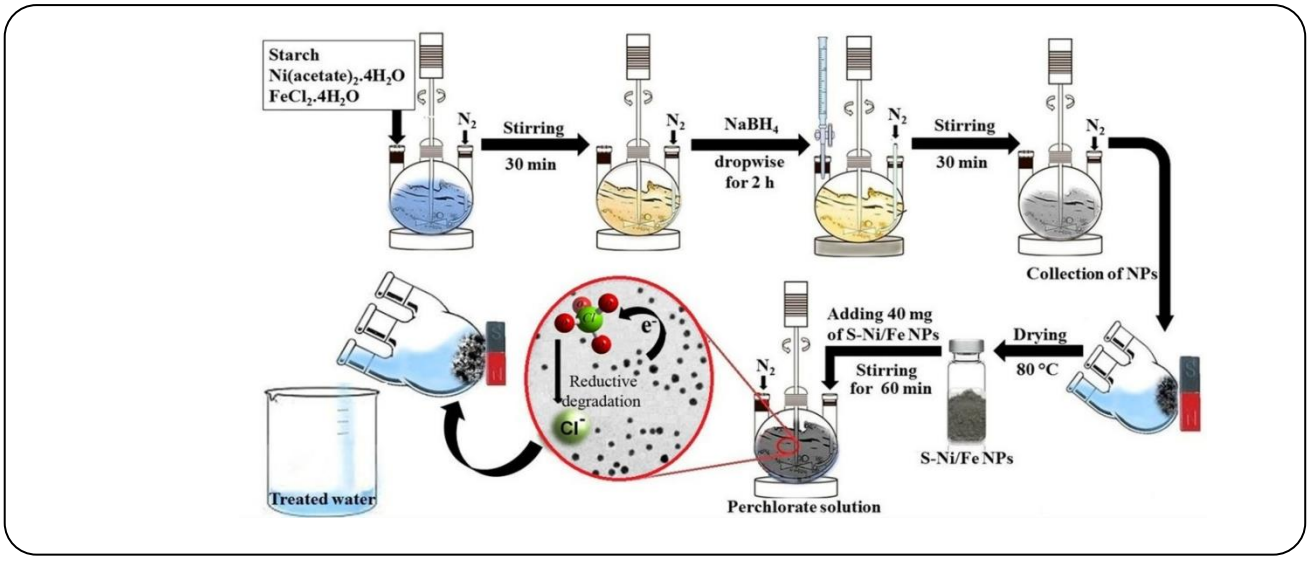


***Scheme 1: Schematic illustration of preparation of S-Ni/Fe NPs and its application in reductive degradation of perchlorate***

The main advantage of RSM is the reduced number of experimental runs needed to provide sufficient information for statistically acceptable results. It is a faster and low-cost method for gathering research results, compared to the classical methods. The main aim of this work was to optimize the conditions to maximize removal of perchlorate. In the design of the experiments, the selection of the factors affecting the desired response is the most important step. Therefore, many factors are considered, which may then be removed because of the negligible impact. In this study, the independent variables pH ($X_1$), the dosage of the S-Ni/Fe NPs ($X_2$), temperature ($X_3$), and time ($X_4$) were investigated using the RSM, and the response was destruction efficiency (%). A face-Centered Composite Design (CCD) with four factors and five coded levels was used to determine the efficiency. After running the experiments and measuring the pectinase activity levels, a second order model including interactions fitted to the response data was used as follow:

$$y = \beta_o + \sum_1^k \beta_i X_i + \sum_1^k \beta_{ii} X_i^2 + \sum_{i<j} \sum B_{ij} X_i X_j + \varepsilon \qquad (5)$$

Where $y$ is the predicted response, $k$ the number of factor variables, $\beta_o$ the model constant, $\beta_i$ the linear coefficient, $X_i$ the factor variable in its coded form, $\beta_{ii}$ the quadratic coefficient, and $\beta_{ij}$ is the interaction coefficient [38]. In the dimensionless coordinate system, the upper and lower levels of the factors are at +1 and -1, respectively. The coordinates of the center point of the design are zero. These coded values of $X_j$ were used to build a regression model to fit the experimental data. The factors and levels were followed according to Table 1.

Fifty additional media optimization experiments were designed in the CCD. The analysis of data and generation of response surface graphics was done by version 10 of the statistical software Design-Expert. The analysis of variance (ANOVA) tables was generated and the effect and regression coefficients of individual linear, quadratic, and interaction terms were determined. The quality of the polynomial model equation was judged statistically by the coefficient of determination $R^2$, and its statistical significance was determined by an F-test.

## RESULTS AND DISCUSSION

### *Characterization of Bimetallic Nanoparticles*

Fig. 1 shows a Scanning Electron Microscopy (SEM) image of the synthesized S-Ni/Fe NPs. It was observed that all the NPs were spherical with an average diameter of 20-50 nm. The Energy-Dispersive X-ray Spectroscopy (EDS) of fresh the S-Ni/Fe NPs (washed with ethanol) was presented in Fig. 2.

The elemental compositions of Fe and Ni in the Ni/Fe NPs were 96.87 and 3.13 wt%, respectively. The crystalline phase of the S-Ni/Fe NPs was determined using an X-ray diffraction pattern (XRD) (Fig. 3). The apparent peaks at the 2θ of 44.64°, 65.16°, and 85.5° indicated the presence of Ni/Fe NPs. The characteristic peak of 2θ= 44.64° indicates the crystallization of $Fe^0$ and $Ni^0$ in S–Fe/Ni NPs [39,40].

***Table 1: The range and levels of the independent variables.***

| Factor | Name | Units | Minimum | Maximum | Coded | Values | Mean |
|---|---|---|---|---|---|---|---|
| $X_1$ | pH | | 3.50 | 9.50 | -1.000=5.00 | 1.000=8.00 | 6.50 |
| $X_2$ | mass of NPs | mg | 10.00 | 90.00 | -1.000=30.00 | 1.000=70.00 | 50.00 |
| $X_3$ | T | °C | 30.00 | 90.00 | -1.000=45.00 | 1.000=75.00 | 60.00 |
| $X_4$ | time | min | 20.00 | 120.00 | -1.000=45.00 | 1.000=95.00 | 70.00 |

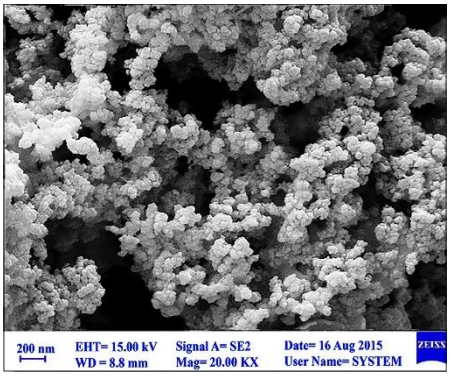


***Fig. 1: (A) Image of laboratory-synthesized S-Ni/Fe NPs obtained with a field-emission scanning electron microscope (SEM) (100.00 KX). Eighty percent particles had diameters less than 100 nm.***

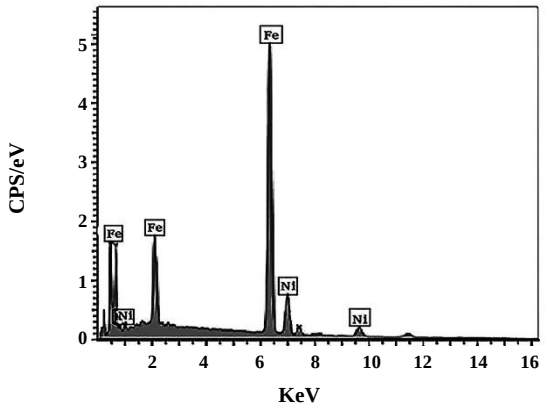


***Fig. 2: EDS spectrum of the S-Ni/Fe NPs (vacuum, 5 × $10^{-7}$ Torr; lens current, 1.8 A; voltage, 20 kV).***

### *Experiment design*

Based on the CCD methodology, thirty tests with different operational conditions were designed (Table 2). The tests were performed and the regression analysis for the reductive destruction of perchlorate ion showed that the data could be modeled by a second-order polynomial equation for perchlorate ion adsorption, described as follows:

$$\%DE = +85.16 - (4.69X_1) + (11.19X_2) + (3.82X_3) + (12.04X_4) - (3.18X_2 \times X_3) - (9.61X_1^2) - (5.63X_2^2) - (2.57X_3^2) - (4.57X_4^2) \quad (6)$$

The analysis of variance (ANOVA) for the response quadratic model was investigated. The values of "Prob>*F*" (*p*-value) less than 0.05 indicate the model terms are significant and the values greater than 0.10 indicate they are not significant. In the present research, $X_1$, $X_2$, $X_3$, $X_4$, $X_2 \times X_3$, $(X_1)^2$, $(X_2)^2$, $(X_3)^2$, and $(X_4)^2$ were the significant model terms. The analysis of variance for the reduced quadratic model for the removal of perchlorate is shown in Table 3.

The Model F-value of 35.35 and the p-value less than 0.0001 implies the model is significant. The lack of fit F-value of 3.29 implies the lack of fit is not significant relative to the pure error. Predicted R-squared represents how good a model predicts a response value. In this work, the predicted R-squared value of 0.86 is in reasonable agreement with the adjusted R-squared value of 0.91. Adequate precision measures the signal-to-noise ratio and a ratio greater than 4 is desirable. For the reduced model, this ratio is 18.89, which indicates an adequate signal. The overall performance of the model is expressed by the R-squared value, as the degree of correlation between the observed and predicted values is expressed by the adjusted R-squared value [41]. For this model, R-squared and adjusted R-squared were 0.94 and 0.91, respectively, which suggests that the model can be used for predicting the process behavior at the design space.

The 2D contour plots and 3D response surface curves were plotted to explain the interactions of the medium components. Each plot showed the effect of two variables, while the other was held at the optimum level. These response surface plots and their respective contour plots provided a visual interpretation of the interaction between

***Table 2: The designed experiments by the CCD method for the destruction process.***

| Run | $X_1$:pH | $X_2$:mass of NPs (mg) | $X_4$:T (°C) | $X_4$:time (min) | DE% |
|---|---|---|---|---|---|
| 1 | 5.00 | 70.00 | 45.00 | 95.00 | 92.75 |
| 2 | 6.50 | 50.00 | 60.00 | 70.00 | 86.56 |
| 3 | 9.50 | 50.00 | 60.00 | 70.00 | 46.87 |
| 4 | 6.50 | 10.00 | 60.00 | 70.00 | 35.43 |
| 5 | 6.50 | 90.00 | 60.00 | 70.00 | 87.87 |
| 6 | 5.00 | 30.00 | 75.00 | 45.00 | 60.87 |
| 7 | 8.00 | 30.00 | 75.00 | 95.00 | 56.87 |
| 8 | 6.50 | 50.00 | 60.00 | 70.00 | 80.7 |
| 9 | 6.50 | 50.00 | 60.00 | 120.00 | 91.87 |
| 10 | 5.00 | 30.00 | 45.00 | 45.00 | 35.87 |
| 11 | 6.50 | 50.00 | 60.00 | 70.00 | 87.34 |
| 12 | 8.00 | 30.00 | 45.00 | 95.00 | 53.87 |
| 13 | 8.00 | 70.00 | 45.00 | 45.00 | 52.87 |
| 14 | 6.50 | 50.00 | 60.00 | 70.00 | 86.76 |
| 15 | 6.50 | 50.00 | 90.00 | 70.00 | 80.76 |
| 16 | 6.50 | 50.00 | 60.00 | 20.00 | 39.87 |
| 17 | 6.50 | 50.00 | 30.00 | 70.00 | 66.98 |
| 18 | 6.50 | 50.00 | 60.00 | 70.00 | 88.87 |
| 19 | 8.00 | 70.00 | 75.00 | 45.00 | 54.54 |
| 20 | 5.00 | 70.00 | 75.00 | 95.00 | 96.23 |
| 21 | 8.00 | 30.00 | 45.00 | 45.00 | 25.98 |
| 22 | 5.00 | 30.00 | 75.00 | 95.00 | 75.43 |
| 23 | 8.00 | 70.00 | 75.00 | 95.00 | 78.87 |
| 24 | 5.00 | 30.00 | 45.00 | 95.00 | 67.76 |
| 25 | 8.00 | 30.00 | 75.00 | 45.00 | 47.77 |
| 26 | 8.00 | 70.00 | 45.00 | 95.00 | 76.87 |
| 27 | 6.50 | 50.00 | 60.00 | 70.00 | 80.76 |
| 28 | 5.00 | 70.00 | 75.00 | 45.00 | 67.65 |
| 29 | 5.00 | 70.00 | 45.00 | 45.00 | 68.23 |
| 30 | 3.50 | 50.00 | 60.00 | 70.00 | 44.54 |

***Table 3: Analysis of variance for the response surface reduced quadratic model.***

| Source | Sum of Squares | df | Mean Square | F Value | p-value Prob > F |
|---|---|---|---|---|---|
| Model | 10767.48 | 9 | 1196.39 | 35.35 | < 0.0001 |
| $X_1$-pH | 527.25 | 1 | 527.25 | 15.58 | 0.0008 |
| $X_2$-mass of NPs | 3003.17 | 1 | 3003.17 | 88.74 | < 0.0001 |
| $X_4$-T | 349.53 | 1 | 349.53 | 10.33 | 0.0044 |
| $X_4$-time | 3476.91 | 1 | 3476.91 | 102.74 | < 0.0001 |
| $X_2X_3$ | 161.86 | 1 | 161.86 | 4.78 | 0.0408 |
| $X_1^2$ | 2535.45 | 1 | 2535.45 | 74.92 | < 0.0001 |
| $X_2^2$ | 868.85 | 1 | 868.85 | 25.67 | < 0.0001 |
| $X_3^2$ | 181.62 | 1 | 181.62 | 5.37 | 0.0312 |
| $X_4^2$ | 573.65 | 1 | 573.65 | 16.95 | 0.0005 |
| Residual | 676.82 | 20 | 33.84 | | |
| Lack of Fit | 614.53 | 15 | 40.97 | 3.29 | 0.0971 |
| Pure Error | 62.29 | 5 | 12.46 | | |
| Cor Total | 11444.30 | 29 | | | |

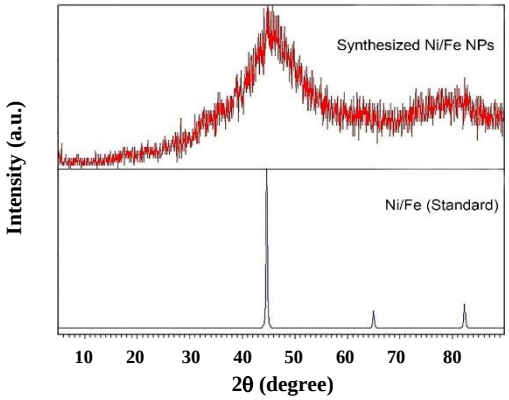


***Fig. 3: XRD patterrn of the S-Ni/Fe NPs.***

two variables. Previous studies reported that the circular contour plots of response surfaces might indicate a negligible interaction between the corresponding variables. An elliptical or saddle nature of the contour plots might indicate the existence of a perfect interaction between these independent variables [42, 43]. The 2D contour plots and 3D response surface curves for the destruction of perchlorate are shown in Fig. 4. As can be seen, the efficiency of destruction is increased when the dosage of the S-Ni/Fe NPs is increased, and it is decreased when there is too much decrease. This observation suggests that there is an interaction between these two factors. At the optimum level, the maximum of destruction efficiency occurred at low pH and high dosage of the S-Ni/Fe NPs. The results show that perchlorate destruction is favored at lower pH with more $H^+$ as a reactant. The nZVI is readily oxidized to ferrous iron, $Fe^{2+}$, by many substances. The electrons required to reduce perchlorate must come from $Fe^0$ either directly or indirectly through the corrosion products, $Fe^{2+}$ ion and hydrogen. $Fe^0$ is a mild reductant, but the presence of nickel along the iron increases the electron production rate in ZVI due to their reduced potential [17, 44]. At higher pH, iron, as an electron producer, showed reducing activity *via* production of iron oxides, and the newly-formed iron oxides cover the $Fe^0$ surfaces to impede further reduction, therefore, perchlorate destruction is not favored at higher pH [45].

A regression model can be used to predict future observations on the response %DE (destruction efficiency) corresponding to particular values of the regress variables. The residuals from the least squares fit to play an important role in judging model adequacy.

The normal probability plot and the residual plot verify all the assumptions for randomness, normality and constant variances of the residuals. The normal plot of

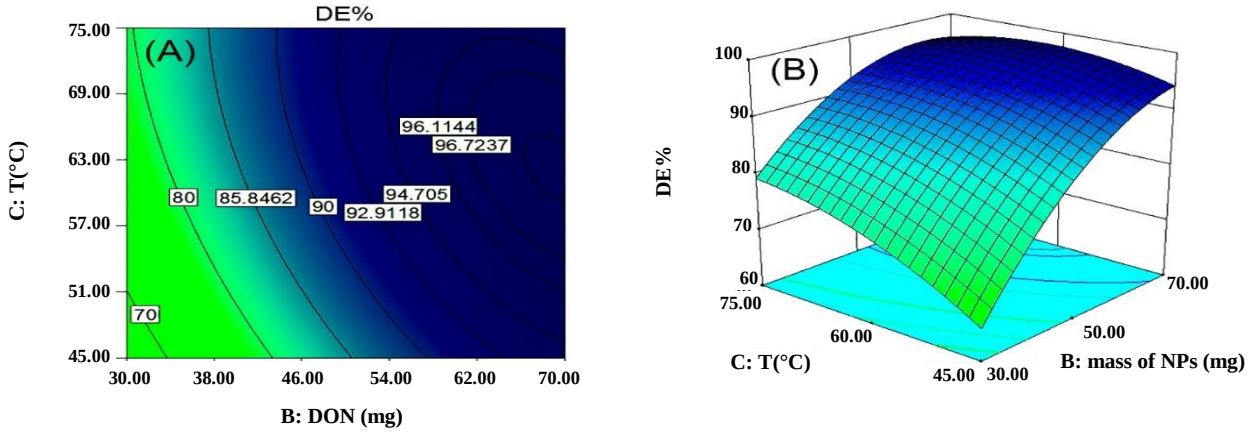


***Fig. 4: Response surface graph of the variation of the destruction efficiency: (A) 2D contour plots, (B) 3D response surface curve.***

residuals is shown in Fig. 5A and Fig. 5B, as the most important diagnostic for the model, the normal probability plot of the residuals, came up by default. A linear pattern demonstrated normality in the error term, i.e., there were no signs of any problems in our data. Fig. 5C and Fig. 5D presents a plot of residuals versus the predicted response. The general impression is that the residuals scatter randomly on the display, suggesting that the variance of the original observation is constant for all values of responses. Both of the plots are satisfactory, so we conclude that the empirical model is adequate to describe the adsorption and destruction efficiency by response surface.

***The optimization of the operating parameters***

The optimization of the process means the finding of value of the operating factors to reach a desired point of the %DE, based on the proposed full factorial model. The optimization study of the experimental results was performed by keeping all responses within desired ranges with the full factorial model. In this study, all variables were within range, and the goals of variables were set "maximize" that was set at %DE of 96.23%. Under the settings, for 50 mL of 10 µg/mL of perchlorate solution, the software predicted a %DE of 96.5% when the optimum value of pH, dosage of NPs, temperature and reaction time be 5.64, 62.86 mg, 70.15 $^0$C, and 90.39 min, respectively. To evaluate the accuracy of the model prediction, further confirmatory experiments were performed under optimum conditions, and a %DE of 97.03% was obtained practically. Also, the destruction efficiency can be improved up to 100% by increasing the time of the process to 110 min.

***Chloride mass balance and reaction completeness***

The reductive destruction of perchlorate to non-toxicity chloride ion is believed to occur via a series of stepwise reactions through chlorate ($ClO_3^-$), chlorite ($ClO_2^-$), hypochlorite ($ClO^-$), and finally chloride ($Cl^-$) (Eqs. 6 to 9).

$$ClO_4^- + 2H^+ + 2e^- \rightarrow ClO_3^- + H_2O \quad (6)$$

$$ClO_3^- + 2H^+ + 2e^- \rightarrow ClO_2^- + H_2O \quad (7)$$

$$ClO_2^- + 2H^+ + 2e^- \rightarrow ClO^- + H_2O \quad (8)$$

$$ClO^- + 2H^+ + 2e^- \rightarrow Cl^- + H_2O \quad (9)$$

In this study, to prove the completion of the process of perchlorate destruction by the S-Ni/Fe NPs, an experiment was conducted using a solution containing 10 µg/mL of the perchlorate under optimal conditions and the amount of produced chloride ion was measured by ion chromatography. According to Fig. 6, and based on the peak area, the concentration of chloride ion was obtained 3.5µg/mL. This value showed that complete destruction of perchlorate to chloride ion stoichiometrically occurred.

***Kinetic study***

The destruction of perchlorate in aqueous solution is a multi-step reaction. Therefore, pseudo-first order kinetic was applied to determine the rate of destruction according to Eq. (10):

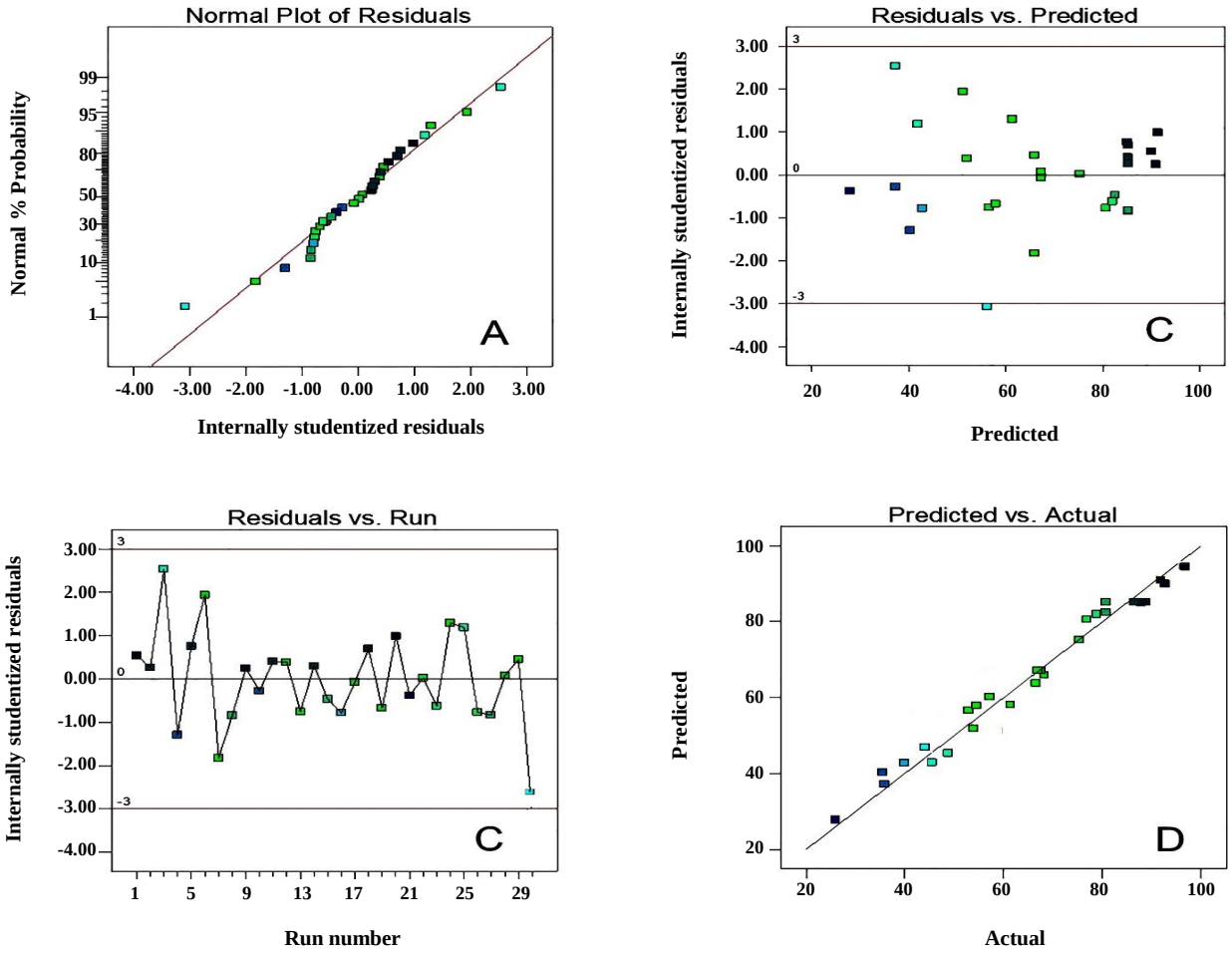


***Fig. 5: Residual diagnostics of the contour surface of the quadratic model. (A), (B) Normal probability of internally studentized residuals. (C), (D) Plot of internally studentized residuals vs. predicted response.***

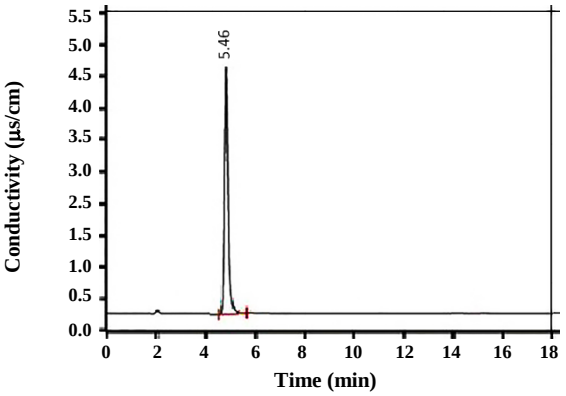


***Fig. 6: Chromatogram of chloride ion resulting from the destruction of perchlorate in optimal conditions. Chromatographic conditions: 6.1006.510 Metrosep a Supp 5-100/4.0. Column (dimensions (mm), 100 × 4.0); mobile phase 1.0 mM $NaHCO_3$, 3.2 mM $Na_2CO_3$; flow rate 0.7 mL $min^{-1}$; injection volume, 20 µL; conductometric detection..***

$$\frac{dC}{dt} = -K_{obs}C \qquad (10)$$

Where $C$ is the concentration of perchlorate (µg/mL); $k_{obs}$ is the measured rate constant ($min^{-1}$) and $t$ is reaction time (min). The pseudo-first-order rate constants were calculated by the method of linear regression. The destruction kinetic for perchlorate was investigated under the optimum conditions and the natural logarithm of $C/C_o$ as a function of time is shown in Fig. 7A.

The slope of the line was $k_{obs}$ and the correlated parameters had a high correlation coefficient ($R^2 > 0.99$). Fig. 7A shows a good fitness of the experimental data for the destruction with the pseudo-first-order kinetic model with the rate constant of 0.0335 $min^{-1}$ at room temperature (25 °C).

Fig. 7B shows an Arrhenius plot of the natural logarithm of the first order rate constant ($k$) versus $1/T$. Data were fitted to the Arrhenius classic equation as follow:

$$\mathrm{Lnk} = \mathrm{LnA} - \mathrm{Ea}/\mathrm{RT} \quad (11)$$

Where $k$ is the rate constant, $A$ is the pre-exponential factor, $E_a$ is the activation energy, $T$ is the temperature (K), and $R$ is the ideal gas constant. The average $E_a$ value was calculated to be 13.07 kJ/mol.

***Application***

To appraise the practical applicability of the proposed method, it was applied to the removal of perchlorate in well water and industrial wastewater. To investigate the effect of matrix and interfering species, 50 mL of 20 µg/mL of perchlorate solution was prepared using well water and after removal of perchlorate under optimum conditions, the mean destruction efficiency was obtained 98.6%. Also, in this research, the removal of perchlorate was carried out on a wastewater sample from perchlorate production factory with a concentration of nearly 200 µg/mL of perchlorate. For this purpose, 5 mL of wastewater was transferred into a 50 mL volumetric flask and was diluted to the mark with distilled water, and then degraded by proposed method under optimum conditions, and destruction efficiency was obtained 97.6%. The results show that the proposed method is applicable to remove perchlorate from wastewater samples.

***Comparative review***

To express the strengths of the study, the proposed method was compared to the other methods that so far have used to remove perchlorate based on reductive destruction. The comparison of the parameters (Table 4) shows that stabilized-Ni/Fe NPs have been better, firstly, because the rate constants of the destruction have been more appropriate due to the relatively lower temperature than the other tests, secondly, the destruction begun with lower activation energy. This high efficiency is due to the presence of starch and Ni. In other words, the presence of starch and Ni can improve the stability and activity of Ni/Fe bimetallic NPs, respectively.

## CONCUSIONS

In this work, we examined the use of S- Fe/Ni NPs for the reductive destruction of perchlorate. The most outstanding findings of the work can be briefly stated as follows: (i) the S-Ni/Fe NPs with a size ranges from 20 to 50 nm were successfully prepared, (ii) perchlorate in the presence of the S-Ni/Fe NPs was destructed to nontoxic chloride ion, (iii) A first-degree order reduced polynomial model established by the full factorial is able to describe the applied chemical reduction with metal nanoparticles well, (iv) based on the model prediction, destruction of perchlorate can reach 97 % that this efficiency can be improved up to 100% by increasing the time of the process to 110 min. Therefore, the S-Ni/Fe NPs can be powerful promising material for reductive destruction of perchlorate from aqueous solutions. Using this method is much faster than other methods of the perchlorate removal.

*Received : Apr. 18, 2019 ; Accepted :Sep. 30, 2019*

## REFERENCES

[1] Nordberg M., Templeton D.M., Andersen O., Duffus J.H., Glossary of Terms Used in Ecotoxicology (IUPAC Recommendations 2009), *Pure. Appl. Chem.*, **81**: 829-970 (2009).

[2] Xie Y., Tao G., Chen Q., Tian X., Effects of Perchlorate Stress on Growth and Physiological Characteristics of Rice (Oryza Sativa L.) Seedlings, *Water. Air. Soil. Poll.*, **225**: 2077-2084 (2014).

[3] Urbansky E.T., Perchlorate as an Environmental Contaminant, *Environ. Sci. Pollut. Res.*, **9:** 187-192 (2002).

[4] Y.Liu Y., Cheng Y., Lv S., Liu C., Lai J., Luo G., Synthesis of Nano-CuI and Its Catalytic Activity in the Thermal Decomposition of Ammonium Perchlorate, *Res. Chem. Intermed.*, **41**: 3885–3892 (2015).

[5] McNabb F.M., Larsen C.T., Pooler P.S., Ammonium Perchlorate Effects on Thyroid Function and Growth in Bobwhite Quail Chicks, *Environ. Toxicol. Chem.*, **23:** 997-1003 (2004).

[6] Amitai Y., Winston G., Sack J., Wasser J., Lewis M., Blount B.C., Valentin-Blasini L., Fisher N., Israeli A., Leventhal A., Gestational Exposure to High Perchlorate Concentrations in Drinking Water and Neonatal Thyroxine Levels, *Thyroid*, **17**: 843-850 (2007).

[7] Burda C., Chen X., Narayanan R., El-Sayed M.A., Chemistry and Properties of Nanocrystals of Different Shapes, *Chem. Rev.*, **105:** 1025-1102 (2005).

[8] Pearson, C.R., Hozalski, R.M., Arnold, W.A., Degradation of Chloropicrin in the Presence of Zero-Valent Iron, *Environ. Toxicol. Chem.*,**24:** 3037-3042 (2005).

[9] Daraei H., Amrane A., Kamali H., Assessment of Phenol Removal Efficiency Synthesized Zero Iron Nanoparticles and Fe Powder Using the Response Surface Methodology, *Iran. J. Chem. Chem. Eng. (IJCCE)*, **36**: 137-146 (2017).

[10] Fu R., Yang Y., Xu Z., Zhang X, Guo X., Bi D., The Removal of Chromium (VI) and Lead (II) from Groundwater Using Sepiolite-Supported Nanoscale Zero-Valent Iron (S-NZVI), *Chemosphere*, **138**: 726-734 (2015).

[11] Cao J., Elliott D, Zhang W.X., Perchlorate Reduction by Nanoscale Iron Particles, *J. Nanopart. Res.*, **7:** 499-506 (2005).

[12] Wang CB., Zhang W.X., Synthesizing Nanoscale Iron Particles for Rapid and Complete Dechlorination of TCE and PCBs, *Environ. Sci. Technol.*, **31**: 2154-2156 (1997).

[13] He F., Zhao D., Preparation and Characterization of a New Class of Starch-Stabilized Bimetallic Nanoparticles for Degradation of Chlorinated Hydrocarbons in Water, *Environ. Sci Technol.*, **39**: 3314-3320 (2005).

[14] Keshipour S., Adak K., Reduction of Nitroaromatics to Amines with Cellulose Supported Bimetallic Pd/Co Nanoparticles, *Iran. J. Chem. Chem. Eng. (IJCCE)*, **37**: 23-31 (2018).

[15] Murray R.W., Nanoelectrochemistry: Metal Nanoparticles, Nanoelectrodes, and Nanopores, *Chem. Rev.*, **108**: 2688-2720 (2008).

[16] Bing Y., Liu H., Zhang L., Ghosh D., Zhang J., Nanostructured Pt-Alloy Electrocatalysts for PEM Fuel Cell Oxygen Reduction Reaction, *Chem. Soc. Rev.*, **39:** 2184-2202 (2010).

[17] Sun S., Murray C., Weller D., Folks L., Moser A., Monodisperse FePt Nanoparticles and Ferromagnetic FePt Nanocrystal Superlattices, *Science*, **287:** 1989-1992 (2000).

[18] Song H.M., Kim W.S., Lee Y.B., Hong J.H., Lee H.G., Hur N.H., Chemically Ordered FePt3 Nanoparticles Synthesized by a Bimetallic Precursor and Their Magnetic Transitions, *J. Mater. Chem.*, **19:** 3677-3681 (2009).

[19] Xiong Z., Zhao, D., Pan, G., Rapid and Complete Destruction of Perchlorate in Water and Ion-Exchange Brine Using Stabilized Zero-Valent Iron Nanoparticles, *Water Res.*, **41:** 3497-3505 (2007).

[20] Kim D.K., Mikhaylova M., Zhang Y., Muhammed M., Protective Coating of Superparamagnetic Iron Oxide Nanoparticles, *Chem. Mater.*, **15:** 1617-1627 (2003).

[21] Chatterjee J., Haik Y, Chen C.J., Polyethylene Magnetic Nanoparticle: A New Magnetic Material for Biomedical Applications, *J Magn. Magn. Mater.*, **246**: 382-391 (2002).

[22] Pardoe H., Chua-Anusorn W., Pierre T.G.S., Dobson J., Structural and Magnetic Properties of Nanoscale Iron Oxide Particles Synthesized in the Presence of Dextran or Polyvinyl Alcohol, *J. Magn. Magn. Mater.*, **225**: 41-46 (2001).

[23] Kataby G., Ulman A., Prozorov R., Gedanken A., Coating of Amorphous Iron Nanoparticles by Long-Chain Alcohols, *Langmuir*, **14**: 1512-1515 (1998).

[24] Liu J., He F., Durham E., Zhao D., Roberts C.B., Polysugar-Stabilized Pd Nanoparticles Exhibiting High Catalytic Activities for Hydrodechlorination of Environmentally Deleterious Trichloroethylene, *Langmuir*, **24**: 328-336 (2008).

[25] He F., Zhao D., Manipulating the Size and Dispersibility of Zerovalent Iron Nanoparticles by Use of Carboxymethyl Cellulose Stabilizers, *Environ. Sci. Technol.*, **41**: 6216-6221 (2007).

[26] He F., Zhao D., Liu J., Roberts C.B., Stabilization of Fe-Pd Nanoparticles With Sodium Carboxymethyl Cellulose for Enhanced Transport and Dechlorination of Trichloroethylene in Soil and Groundwater, *Ind. Eng. Chem. Res.*, **46**: 29-34 (2007).

[27] Yazdanbakhsh A.R., Daraei H., Rafiee M., Kamali H., Performance of iron Nano Particles and Bimetallic Ni/Fe Nanoparticles in Removal of Amoxicillin Trihydrate from Synthetic Wastewater, *Water Sci. Technol.*, **73**: 2998-3007 (2016).

[28] Logan B.E., LaPoint D., Treatment of Perchlorate- and Nitrate-Contaminated Groundwater in an Autotrophic, Gas Phase, Packed-Bed Bioreactor, *Water Res.*, **36**: 3647-3653 (2002).

[29] McCarty P.L, Meyer T.E., Numerical Model for Biological Fluidized-Bed Reactor Treatment of Perchlorate-Contaminated Groundwater, *Environ. Sci. Technol.*, **39**: 850-858 (2005).

[30] Xiong Z., Dimick P., Zhao D., Kney A., Tavakoli J., Removal of Perchlorate from Contaminated Water Using a Regenerable Polymeric Ligand Exchanger, *Sep. Sci. Technol.*, **41**: 2555-2574 (2006).

[31] Chen W., Cannon F.S., Rangel-Mendez J.R., Ammonia-tailoring of GAC to enhance perchlorate removal. II: Perchlorate adsorption, *Carbon*, 43: 581-590 (2005).

[32] Yoon J., Yoon Y., Amy G., Cho J., Foss D., Kim T.H., Use of Surfactant Modified Ultrafiltration for Perchlorate ($ClO_4^-$) Removal, *Water Res.*, **37**: 2001-201 (2001).

[33] Moore A.M., De Leon C.H., Young T.M., Rate and Extent of Aqueous Perchlorate Removal by Iron Surfaces, *Environ. Sci. Technol.*, **37:** 3189-3198 (2003).

[34] Cao J., Elliott D., Zhang W., Perchlorate Reduction by Nanoscale Iron Particles, *J Nanopart. Res.*, **7**: 499-506 (2005).

[35] Lien H.L., Yu C.C., Lee Y.C., Perchlorate Removal by Acidified Zero-Valent Aluminum and Aluminum Hydroxide, *Chemosphere,* **80**: 888-893 (2010).

[36] Moore A.M., De Leon, C.H., Young, T.M., Rates and Extent of Aqueous Perchlorate Removal by Iron Surfaces, *Environ. Sci. Technol.*, **37:** 3189-3198 (2003).

[37] Nabar G., Ramachandran C., Quantitative Determination of Perchlorate Ion in Solution, *Anal. Chem.*, **31:** 263-265 (1959).

[38] Lin Y., Chen Z., Megharaj M., Naidu R., Degradation of Scarlet 4BS in Aqueous Solution Using Bimetallic Fe/Ni Nanoparticles, *J. Colloid. Interface Sci.*, **381:** 30-35 (2012).

[39] Geng B., Jin Z., Li T., Qi X., Kinetics of Hexavalent Chromium Removal from Water by Chitosan-$Fe^0$ Nanoparticles, *Chemosphere*, **75:** 825-830 (2009).

[40] Montgomery S.L., Permian Bone Spring Formation: Sandstone Play in the Delaware Basin, Part II-Basin, *AAPG Bulletin*, **81:** 1423-1434 (1997).

[41] Gao H., Liu M., Liu J., Dai H., Zhou X., Liu X., Zhuo Y., Zhang W., Zhang L., Medium Optimization for the Production of Avermectin B1a by Streptomyces Avermitilis 14-12A Using Response Surface Methodology, *Bioresour. Technol.*, **100**: 4012-4016 (2009).

[42] Su J.J., Zhou Q., Zhang H.Y., Li Y.Q., Huang X.Q., Xu Y.Q., Medium Optimization for Phenazine-1-Carboxylic Acid Production by a Gaca Qscr Double Mutant of Pseudomonas sp. M18 Using Response Surface Methodology, *Bioresour. Technol.*, **101**: 4089-4095 (2010).

[43] Gu B., Dong W., Brown G.M., Cole D.R., Complete Degradation of Perchlorate in Ferric Chloride and Hydrochloric Acid Under Controlled Temperature and Pressure, *Environ. Sci. Technol.*, **37**: 2291-2295 (2003).

[44] Chen J.L., Al-Abed S.R., Ryan J.A., Li Z., Effects of pH on Dechlorination of Trichloroethylene by Zero-Valent Iron, *J. Hazard. Mater.*, **83**: 243-254 (2001).

[45] Srinivasan R., Sorial G.A., Treatment of Perchlorate in Drinking Water: A Critical Review, *Sep. Pur Technol.*, **69**: 7-21 (2009).